Appl. Phys. B 68, 983–987 (1999) / DOI 10.1007/s003409900010

Applied Physics B
Lasers
and Optics

Photorefractive effects in long, narrow BSO crystals with applied electric field

G. Cedilnik[1], M. Esselbach[1], A. Kiessling[1], R. Kowarschik[1], E. Nippolainen[2], A.A. Kamshilin[2], V.V. Prokofiev[2]

[1] Institute of Applied Optics, Friedrich-Schiller-University Jena, Max-Wien-Platz 1, D-07743 Jena, Germany
(Fax: +49-3641/947652, E-mail: cedilnik@pinet.uni-jena.de)
[2] Department of Physics, University of Joensuu, P.O. Box 111, FIN-80101, Joensuu, Finland

Received: 18 November 1998/Revised version: 3 February 1999/Published online: 7 April 1999

Abstract. In a photorefractive $Bi_{12}SiO_{20}$ crystal with high applied electric ac field of square-wave shape a fast two-wave coupling response (less than 1 s) and a slow hologram readout decay (minutes) was found for a wavelength of 633 nm. This can be explained by electron–hole transport with two trap levels. An intensity dependence of the slower complementary grating was found. Illuminating with the readout wave without applied electric field leads to a very slow grating decay (many hours).

PACS: 42.65.Hw; 42.70.Ln; 42.40.Ht

Photorefractive crystals of the sillenite family, i.e., $Bi_{12}SiO_{20}$ (BSO), $Bi_{12}GeO_{20}$ (BGO), and $Bi_{12}TiO_{20}$ (BTO) are of special interest for wave coupling effects, phase conjugation, and optical storage due to their relatively high sensitivity [1, 2]. The buildup of photorefractive gratings can be strongly enhanced by application of an electric field to the crystal. To maximize the energy coupling, ac fields [3, 4] or dc fields in conjunction with moving gratings [5–7] are used. The ac method has the advantage of a simpler setup and of showing a constant amplification over a broad range of intensities without resonant behavior. The square-wave electric field used in this work yields the largest enhancement of grating formation for a given field amplitude [4].

Nominally undoped crystals of BSO and BGO are typically used within the green–blue spectral range (for example 514 nm) [2]. At 633 nm the sensitivity for photorefractive processes is found 1–2 orders of magnitude smaller. On the other hand nominally undoped crystals were successfully used for writing holographic gratings with 785 nm wavelength [8]. It is known that nominally undoped crystals can show differing photorefractive properties. This is because upon production of the crystals, depending on purity of ingredients and pulling conditions, different impurities and crystal defects establish in the crystal. For example, a content of Cr with 1×10^{-4} wt. % weight percents was found to change the photorefractive properties [9]. The spectral sensitivity of sillenites can be changed by (purposely or accidentally) doping [10]. Different samples of nominally pure BSO were shown to have different signs of the photocarriers [11] and different photorefractive behavior [12].

The simultaneous appearance of electron and hole conduction which is observed mostly in nominally undoped crystals [13] can lead to photorefractive gratings with different signs compensating each other. This can be used for hologram fixing with extended readout times compared to the writing times (for example 150-fold) in BSO [8, 14, 15] and other sillenites [16]. The band transport model of Kukhtarev [17] was expanded to describe the buildup dynamics and stationary amplitudes of electron and hole gratings and of the resulting space-charge field which is important for the diffraction efficiency. Different behaviors can be derived from models assuming electron and hole conduction with common trap centers [18] and with different trap centers for electrons and holes [13]. Both cases are compared in [19, 20]. Electron and hole excitation and recombination depend on the wavelength. So, for example, in [8] electron–hole competition effects were observed at 785 nm but not at 514 nm in one BSO sample.

For this work a crystal of nominally pure BSO with long and narrow geometrical shape ("fiber-like") was used. With a wavelength of 633 nm two-wave coupling and readout of stored holograms are investigated. The observations can be explained by electron–hole gratings with different trap levels for electrons and holes. An extraordinary robustness against erasure by illumination was found that allows readout of a grating even after several hours of illumination with white light.

1 Experiment

1.1 Used crystal and optical parameters

The BSO crystal used in this work was grown at the University of Joensuu, Finland, from a stoichiometric melt with the Czochralski method in air atmosphere. The summary content of 13 controlled impurities (e.g. Ba, V, Fe, Co, Cu, Mn, Ni, Ti, Cr) in the starting materials did not exceed 5×10^{-4} wt. %. It was cut in a fiber-like shape, this means

Dedicated to Prof. Dr. Eckard Krätzig on the occasion of his 60th birthday.

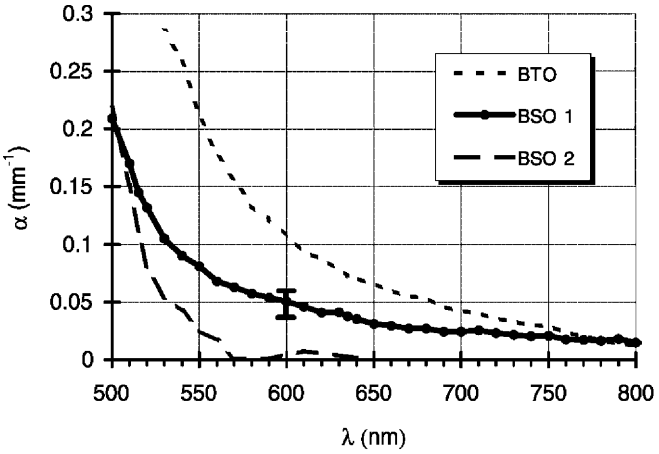

Fig. 1. Absorption spectrum of the fiber-like BSO crystal (BSO 1) compared with two other samples

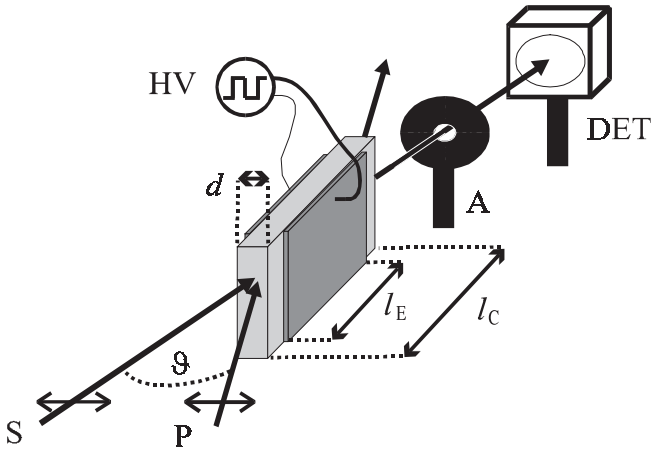

Fig. 2. Two-wave mixing setup with a BSO crystal, high voltage power supply HV, aperture A, and photodetector DET. Signal wave S and pump wave P are both polarized in the plane of incidence (indicated by *arrows*). Crystal dimensions are $d = 1.45$ mm and $l_C = 10.8$ mm, and electrode length $l_E = 8.1$ mm. Electrodes are made from evaporated silver

large along the propagation axis (10.85 mm, [110] crystallographic direction) and small along the other directions (1.45 mm along $[1-11]$ and 4.85 mm along $[-112]$). Silver electrodes are evaporated on the $(1-11)$ surfaces. The short distance of the electrodes of 1.45 mm allows large applied electric fields inside the crystal with moderate applied voltages.

Some optical parameters of the crystal were measured at a wavelength of 633 nm. An optical activity $\rho = 21.1°/\text{mm}$ was found which agrees well with the corresponding values of other samples [2, 21, 22]. The (unclamped) electrooptic coefficient r_{41} was determined by measuring the transmission of linearly polarized light through a system of polarizer, crystal, and analyzer [23]. The value $r_{41} = 4.6 \times 10^{-12}\,\text{m/V}$ $(\pm 0.1 \times 10^{-12}\,\text{m/V})$ also lies within the range of values given elsewhere [2, 21, 22, 24]. An important parameter for the sensitivity of a photorefractive crystal is its optical absorption.

In Fig. 1 the absorption spectrum of the fiber-like BSO crystal ("BSO 1") is compared with the spectra of a nominally undoped bulk BSO crystal ("BSO 2") produced in Trnovo, Slovakia, and a nominally undoped BTO sample. Fresnel losses from single reflections on both surfaces were taken into account. BSO 1 shows an increased absorption in the red and near-infrared spectral region compared to the BSO 2.

1.2 Photorefractive properties

1.2.1 Experimental condition. The photorefractive properties of the crystal with applied electric ac field (±4 kV, 50 Hz) of square-wave shape were determined with the two-wave mixing arrangement shown in Fig. 2. All measurements were performed with the incident light polarized in the plane of incidence. The unexpanded beam of a He-Ne laser (Gaussian intensity profile with 1.9 mm diameter) was used. The incidence angle $\vartheta = 3.8°$ leads to a grating frequency $K = 9.5\,\mu\text{m}^{-1}$ of the holographic grating.

The long interaction length ($l_C = 10.8$ mm) and high applied electric field (±27.6 kV/cm with ±4 kV applied voltage and electrode distance $d = 1.45$ mm) lead to a strong enhancement of the beam coupling process. The two-wave mixing gain G is defined by the ratio $P_S(U)/P_S(0)$ of the signal powers behind the crystal with electric field switched on ($P_S(U)$) and off ($P_S(0)$). Gain factors of up to $G = 1000$, decreasing to 400 at the steady state were found (incident powers $P_{P0} = 0.36$ mW and $P_{S0} = 0.08\,\mu$W of pump and signal wave, respectively). For lower power ratios P_{P0}/P_{S0} the gain is limited due to depletion of the pump wave.

With the arrangement given in Fig. 2 the dynamics of the signal power P_S behind the crystal during writing with both waves was measured. All measurements in BSO with applied electric field show fast changes of the gain or of the diffracted intensity at the moment of reversal of the square-wave field (that takes ≈ 1 ms with the used power supply). Such peaks were found before in BTO [25]. The reason is a change of the polarization state while the modulo of the electric field inside the crystal decreases and reaches zero. The changed polarization state can lead to an increased or decreased diffraction efficiency leading to peaks in positive or negative direction. In the given configuration with BSO, the polarization stays linear in the field-free case and the polarization angle rotates 229° during propagation inside the crystal which leads to a reduced diffraction efficiency. Therefore, with the configuration used in this work the peaks always have negative sign. They reduce the signal as far as 50% during the field reversal. In the following figures of this work these peaks are removed and the gaps are interpolated.

1.2.2 Writing. The buildup of P_S for different incident powers of the writing beams is shown in Fig. 3. For each intensity one can see a fast increase of P_S which reaches a maximum. For higher intensities (Figs. 3b and 3c) a slower decrease of P_S follows. All three curves of Fig. 3 can be very well described by the square-sum of two exponential functions with different buildup times τ_1, τ_2 and amplitudes A_1, A_2:

$$P_S = \left(A_1(1-\exp\{-t/\tau_1\}) + A_2(1-\exp\{-t/\tau_2\})\right)^2 . \qquad (1)$$

The first part in (1) has the higher amplitude and is responsible for the initial increase, and the second part has the opposite sign and thus is responsible for the following decrease of the signal power. Due to the dominant electron photoconduc-

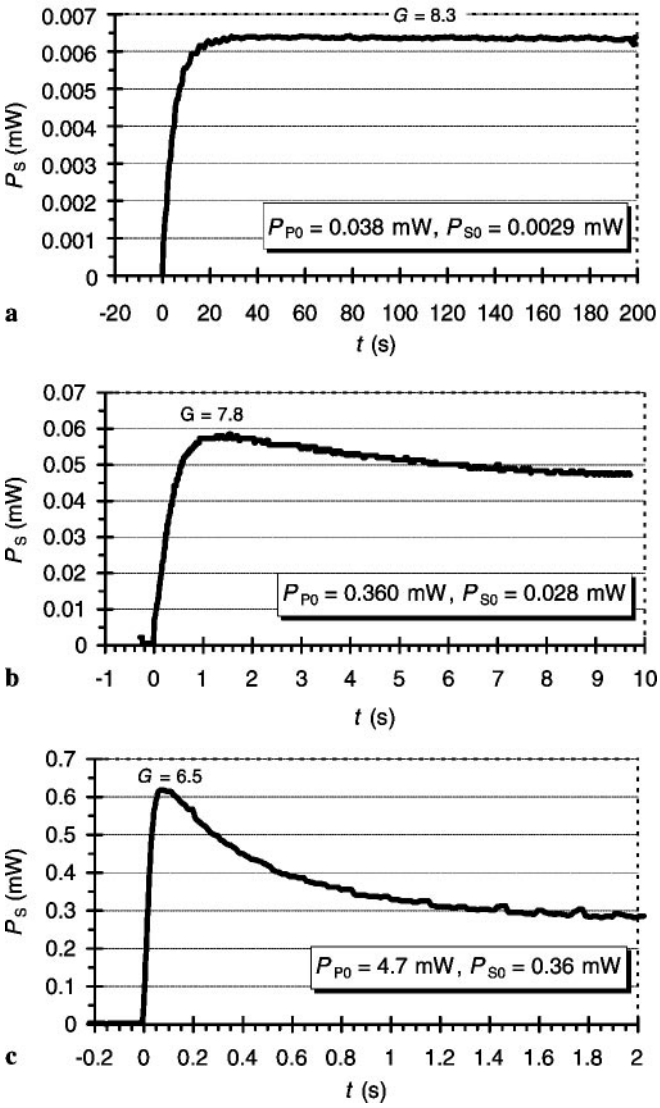

Fig. 3. Buildup of the signal intensity (measured behind the crystal) in the two-wave mixing arrangement after switching on the waves at $t = 0$ for different incident pump and signal powers P_{P0} and P_{S0}. The pump-to-signal intensity ratios are constant. The maximum gain G is given for each intensity

tion found in undoped BSO [26] a grating based on electron transport processes is assumed for the first part, whereas hole transport processes are responsible for the complementary second part. The values for τ_1, τ_2, and the ratio A_2/A_1 are shown in Table 1 from fitting to the experimental data.

The stationary signal intensity was measured in dependence on the incidence angle ϑ (Fig. 4) with beam powers $P_P = 0.31\,\text{mW}$, $P_S = 5.7\,\mu\text{W}$ and an applied voltage of

Table 1. Values for τ_1, τ_2, and the ratio A_2/A_1 from fitting to the experimental data

$P_{P0} + P_{S0}$/mW	τ_1/s	τ_2/s	A_2/A_1
0.041	4.0	—	0
0.39	0.28	6.0	−0.24
5.1	0.017	0.50	−0.58

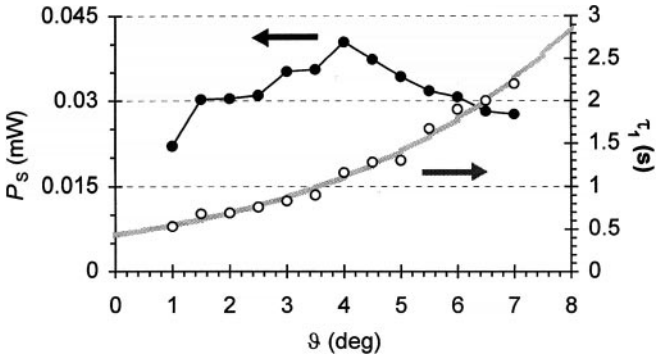

Fig. 4. Dependence of the stationary signal power P_S and response time τ_1 on the incidence angle ϑ in the two-wave mixing arrangement. Angles $\vartheta = 1°$ to $7°$ correspond to $\Lambda = 36\,\mu\text{m}$ to $5.2\,\mu\text{m}$ ($K = 0.17\,\mu\text{m}^{-1}$ to $1.2\,\mu\text{m}^{-1}$) of the grating spacing (grating frequency). Incident powers were $P_{P0} = 0.31\,\text{mW}$ for the pump beam and $P_{S0} = 5.7\,\mu\text{W}$ for the signal beam, applied voltage $U_{HV} = \pm 3.0\,\text{kV}$ at 50 Hz. The *grey line* is an exponential fit, the *black line* connects experimental points

$U_{HV} = \pm 3.0\,\text{kV}$ at 50 Hz. A maximum is found for $\vartheta = 4°$. The response time τ_1 is found to increase with increasing incidence angle. This can be well fitted by an exponential law (grey line).

1.2.3 Readout. After writing the photorefractive grating for 5 min with both waves the signal wave was switched off at $t = 0$. The writing powers were $P_{P0} = 0.36\,\text{mW}$ and $P_{S0} = 0.029\,\text{mW}$ (as in Fig. 3b). Figure 5 shows the power P_P' that is diffracted from the pump wave in the direction of the signal wave (different time-scales in Fig. 5a and b). One can see first a decrease of P_P' within 2.5 s. Then the power increases

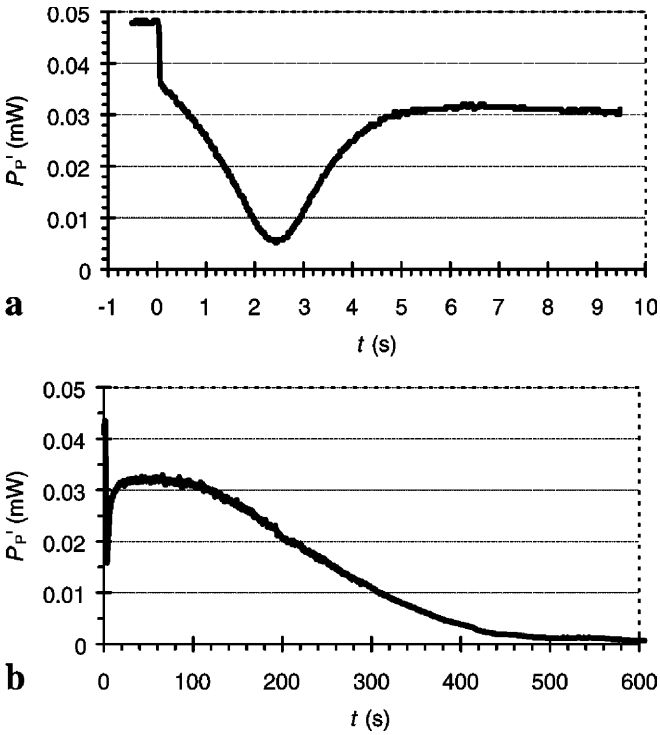

Fig. 5. Intensity of diffracted light after writing a grating for 5 min and switching off the signal wave at $t = 0$ in a short time-scale (**a**) and a long time-scale (**b**). Writing powers were $P_{P0} = 0.36\,\text{mW}$ and $P_{S0} = 0.028\,\text{mW}$

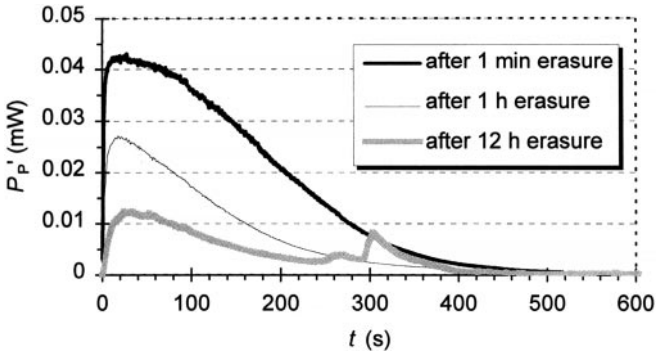

Fig. 6. Intensity of the diffracted light after writing a grating for 5 min and erasing for different time periods (illuminating with pump wave without applied electric field). The reason for the increase in the 12-h curve after 250 s and 300 s is not known

with approximately the same rate forming a curve with a relatively symmetric "dip". After that the signal intensity reaches a maximum with a diffraction efficiency nearly as high as the one at $t = +0$. For about 60 s the intensity stays at that maximum with little change, then decreases again with a much slower rate (decrease to $1/e$ in about 350 s). Such a behavior was observed with all three writing intensities from Fig. 3, even with the low intensity where no decrease of the gain is seen upon writing (Fig. 3a).

We note that the first decrease (and the following increase) is slower than the fast buildup with time constant τ_1 in Fig. 3b. Such a long readout with the large diffraction efficiency was observed only after writing periods of at least 5 min. As is clearly seen in Fig. 5b, the second decrease is much slower than the decrease during writing with the time constant t_2 (Fig. 3b).

1.2.4 Erasure. A remarkable feature is the insensitivity of the BSO 1 crystal against erasure by illumination without electric field. The holographic grating was first written by signal and pump wave with applied electric field for 5 min ($P_{P0} = 0.36$ mW and $P_{S0} = 0.029$ mW, as in Fig. 3b) where saturation of the relevant processes is expected. After that the signal wave and the electric field were switched off. The crystal was illuminated by the pump wave only for different time periods. After that the electric field was switched on again and the diffracted pump intensity was measured (Fig. 6). One can see an appreciable grating still present even after 12 h of illumination. We note that in the time without applied electric field no diffraction of the pump wave could be seen.

A comparable insensitivity against optical erasure without applied field was also observed upon illumination with white light (halogen lamp) of same intensity. On the other hand, the grating formation process was found to take place by illumination of the crystal with both waves without electric field with a rate and amplitude in the order of the case where the ac electric field is on.

2 Discussion

2.1 Material properties

Measurement of the optical properties of the BSO 1 crystal show large differences between two different nominally pure crystals. Although optical activity and electrooptic coefficient lie in the usual region the absorption spectrum differs considerably between BSO 1 and BSO 2 with the first one having a much higher absorption in the red up to the infrared spectral range. The reason is different impurities and crystal defects that have to be specified.

2.2 Photorefractive properties

2.2.1 Writing. The development of the two-wave coupling signal power P_S upon illumination in BSO 1 shows two exponentials of opposite sign with different time constants (1). This behavior can be explained by the formation of two complementary gratings due to electron and hole conduction with separate trap levels for both charge carrier types. The time constants for both parts (Table 1) are approximately inversely proportional to the total optical power. Their relative contributions depend on the intensity. An intensity dependence of the two-wave coupling coefficient with applied electric square-wave field was found in doped BTO:Cd crystals [27]. It results from additional shallow traps. The model there is based on one charge carrier type. For description of the effects in the BSO 1 sample it seems to be necessary to include shallow traps either for one or for both types of charge carriers.

The response time τ_1 of the process increases with increasing spatial frequency of the grating according to [19].

The stationary signal power shows a small dependence on the spatial frequency with a maximum at $K = 0.69\,\mu\text{m}^{-1}$ ($\vartheta = 4°$). This behavior agrees well with the calculated curve in [4] for an applied electric square-wave field in BSO where the maximum is found at the same spatial frequency region. These calculations are based on the Kukhtarev model assuming single charge carrier type and single trap level which is also valid for the two-carrier, two-trap-level model in the initial time where one type of gratings has a much higher buildup rate.

The decrease of the signal power after some time in Fig. 3 is observed only for sufficiently high incident powers. Such a behavior was also mentioned in [16] for BTO ($\lambda = 633$ nm, $K = 30\,\mu\text{m}^{-1}$) though the reason for this is still unclear.

2.2.2 Readout. Upon readout with applied electric ac field immediately after writing, the diffracted intensity shows an oscillation which is also explained in the model of two charge carrier types. The first decrease is due to the decay of the fast (electron) charge grating, the second slow decay results from the decay of the remaining complementary (hole) grating. The readout can also be described by the square sum of two exponential functions, similar to (1). But with this the symmetry in the dip (Fig. 5a) is not obtained.

Another deviation from the theory is seen in our measurements. The theory predicts a decrease of the diffracted power to a minimum value of zero after the first decrease. This is not reached in Fig. 5. Such a deviation was also found and discussed in [8]. There it was supposed that a phase shift of the complementary gratings or a complex relaxation rate (leading to anisotropic relaxation) could lead to a non-complete compensation. We propose another explanation based on self-enhancement and the optical activity of the material. Self-enhancement of the grating results from interference of the

reading beam with the diffracted wave [28, 29]. The grating strength is expected to be strongly inhomogeneous inside the crystal due to wave-coupling during writing. Self-enhancement (and intensity decrease in the crystal depth due to absorption) leads to an inhomogeneous decay of the gratings inside the crystal during readout. Therefore exact compensation of the gratings cannot occur simultaneously in the whole crystal. Diffracted parts from different depths in the crystal cannot add to zero because of more or less different polarization angles (or states) due to the optical activity. So diffraction efficiency never reaches zero at this minimum.

An applied electric field strongly enhances the diffraction efficiency at readout. No diffracted signal could be seen when the voltage was off. This enhancement was described for BTVO [30] before. There a modulated conductivity according to the modulated donor and trap occupation was proposed as explanation which leads to an additional charge accumulation and thus to a stronger diffraction grating.

2.2.3 Erasure. The storage time τ_S for large grating periods (as is the case here with $\Lambda = 10\,\mu m$) in the one charge carrier model is given by the dielectric relaxation time of the crystal:

$$\tau_S = \varepsilon_0 \varepsilon / \sigma \,, \tag{2}$$

where $\varepsilon_0 \varepsilon$ is the permittivity of the crystal and σ the conductivity. Storage times in darkness of more than 20 h were reported in undoped BSO [1, 16]. Illumination increases the conductivity by creating additional mobile charge carriers and thus the storage time decreases. In the case of compensated gratings (when no electric field is applied), the space-charge field that forces mobile charge carriers to homogenize the charge distribution is missing. This can explain the much smaller decay rate found upon illumination of the crystal without applied electric field. This characteristic of the BSO crystal makes it possible to successively write holograms without applied electric field where nearly no erasing of the previously written holograms is expected. These holograms can be read by application of an electric field for relatively long times as shown in Fig. 5b.

3 Summary

We reported about a nominally pure BSO crystal with an increased absorption of red light compared to another nominally pure BSO crystal. This crystal shows a strong photorefractive response at a wavelength of 633 nm with an electric square-wave field applied to the crystal. In a two-wave coupling arrangement the buildup of a complementary grating was seen. This can be explained by two-trap-level, electron–hole conduction. A dependence of the amplitude of the complementary grating on the writing intensity was found but could not be explained. The amplitude of the primary grating over spatial frequency shows a maximum as the theory for single-charge-carrier, single-trap model describes. The two complementary gratings lead to a fast increase of the gain due to the fast primary grating buildup ($\tau_1 = 0.28$ s at 0.39 mW incident power) and a much slower readout decay due to the slower decay of the secondary grating (falling to $1/e$ in 350 s).

When illuminating the crystal without applied electric field, a much slower grating decay was found. After 12 h illumination, the diffraction efficiency reaches 25% of the value without illumination which corresponds to a decrease of the grating amplitude to 50%. Erase of the holographic grating within minutes could only be reached by simultaneous illumination and application of an electric field.

References

1. J.P. Huignard, F. Micheron: Appl. Phys. Lett. **29**, 591 (1976)
2. M.P. Petrov, S.I. Stepanov, A.V. Khomenko: *Photorefractive Crystals in Coherent Optical Systems* (Springer, Berlin, Heidelberg 1991)
3. S.I. Stepanov, M.P. Petrov: Opt. Commun. **53**, 292 (1985)
4. K. Walsh, A.K. Powell, C. Stace, T.J. Hall: J. Opt. Soc. Am. B **7**, 288 (1990)
5. J.P. Huignard, A. Marrakchi: Opt. Commun. **38**, 249 (1981)
6. S.I. Stepanov, V.V. Kulikov, M.P. Petrov: Opt. Commun. **44**, 19 (1982)
7. Ph. Refregier, S. Solymar, H. Rajbenbach, J.P. Huignard: J. Appl. Phys. **58**, 45 (1985)
8. M.C. Bashaw, T.-P. Ma, R.C. Barker, S. Mroczkowski, R.R. Dube: Phys. Review B, **42**, 5641 (1990)
9. E.V. Mokrushina, A.A. Nechitailov, V.V. Prokofiev: Opt. Commun. **123**, 592 (1995)
10. S. Riehemann, F. Rickermann, V.V. Volkov, A.V. Egorysheva, G. von Bally: J. Nonl. Opt. Phys. Mater. **6**, 235 (1997)
11. G. Pauliat, M. Allain, J.C. Launay, G. Roosen: Opt. Commun. **61**, 321 (1987)
12. L.M. Bernardo, J.C. Lopes, O.D. Doares: Appl. Opt. **29**, 12 (1990)
13. M.C. Bashaw, T.-P. Ma, R.C. Barker, S. Mroczkowski, R.R. Dube: J. Opt. Soc. Am. B **7**, 2329 (1990)
14. J.P. Herriau, J.P. Huignard: Appl. Phys. Lett. **49**, 1140 (1986)
15. A. Delboulbe, C. Fromont, J.P. Herriau, S. Mallick, J.P. Huignard: Appl. Phys. Lett. **55**, 713 (1989)
16. M. Miteva, L. Nikolova: Opt. Commun. **67**, 192 (1988)
17. N.V. Kukhtarev: Sov. Tech. Phys. Lett. **2**, 438 (1976)
18. F.P. Strohkendl, R.W. Hellwarth: J. Appl. Phys. **62**(6), 2450 (1987)
19. G.C. Valley: J. Appl. Phys. **59**(10), 3363 (1986)
20. M.C. Bashaw, T.-P. Ma, R.C. Barker: J. Opt. Soc. Am. B **9**, 1666 (1992)
21. L. Solymar, D.J. Webb, A. Grunnet-Jepsen: Prog. Quantum Electron. **18**, 5 (1994)
22. A. Marrakchi, R.V. Johnson, A.R. Tunguay, Jr.: J. Opt. Soc. A **3**, 321 (1986)
23. G. Cedilnik, M. Esselbach, A. Kiessling, R. Kowarschik, A.A. Kamshilin, E. Shamonina, K.H. Ringhofer: J. Appl. Phys. **85**(3), 1317 (1999)
24. A. Grunnet-Jepsen, I. Aubrecht, L. Solymar: J. Opt. Soc. Am. B **12**, 921 (1995)
25. E. Shamonina, K.H. Ringhofer, B.I. Sturman, V.P. Kamenov, G. Cedilnik, M. Esselbach, A. Kiessling, R. Kowarschik, A.A. Kamshilin, V.V. Prokofiev, T. Jaaskelainen: Opt. Lett. **23**, 1435 (1998)
26. R.E. Aldrich, S.L. Hou, M.L. Harvill: J. Appl. Phys. **42**(1), 493 (1971)
27. F. Rickermann, S. Riehemann, K. Buse, D. Dirksen, G. von Bally: J. Opt. Soc. Am. B **13**, 2299 (1996)
28. M. Segev, A. Kewitsch, A. Yariv, G.A. Rakuljic: Appl. Phys. Lett. **62**, 907 (1993)
29. M. Jeganathan, M.C. Bashaw, L. Hesselink: Opt. Lett. **19**, 1415 (1994)
30. S.M. Shandarov, O.V. Kobozev, A.V. Reshetko, M.G. Krause, V.V. Volkov, Y.F. Kargin: Ferroelectrics **202**, 257 (1997)